Chin. Phys. Lett. **39**, 047402 (2022) **Express Letter**

Screening Promising CsV_3Sb_5-Like Kagome Materials from Systematic First-Principles Evaluation

Yutao Jiang(姜昱韬)[1,2†], Ze Yu(喻泽)[1,2†], Yuxin Wang(王郁欣)[1,2], Tenglong Lu(芦腾龙)[1,2], Sheng Meng(孟胜)[1,2,3*], Kun Jiang(蒋坤)[1,3*], and Miao Liu(刘淼)[1,3,4*]

[1]*Beijing National Laboratory for Condensed Matter Physics, Institute of Physics, Chinese Academy of Sciences, Beijing 100190, China*
[2]*School of Physical Sciences, University of Chinese Academy of Sciences, Beijing 100190, China*
[3]*Songshan Lake Materials Laboratory, Dongguan 523808, China*
[4]*Center of Materials Science and Optoelectronics Engineering, University of Chinese Academy of Sciences, Beijing 100049, China*

(Received 1 March 2022; accepted 7 March 2022; published online 11 March 2022)

The CsV_3Sb_5 kagome lattice holds the promise for manifesting electron correlation, topology and superconductivity. However, by far only three CsV_3Sb_5-like kagome materials have been experimentally spotted. We enlarge this family of materials to 1386 compounds via element species substitution, and the further screening process suggests that 28 promising candidates have superior thermodynamic stability, hence they are highly likely to be synthesizable. Moreover, these compounds possess several unique electronic structures, and can be categorized into five non-magnetic and three magnetic groups accordingly. It is our hope that this work can greatly expand the viable phase space of the CsV_3Sb_5-like materials for investigating or tuning the novel quantum phenomena in kagome lattice.

DOI: 10.1088/0256-307X/39/4/047402

In condensed matter physics, kagome lattice serves as an important quantum material system to manifest/investigate the interplay between electron correlation, topology, and lattice geometry.[1,2] For example, kagome lattice is featuring novel electronic structures, such as the flat band, Dirac cone, van Hove points, etc., owing to its special lattice geometry.[3] By far, several materials have been discovered to be able to host the kagome lattices and novel kagome physics, e.g., the Fe kagome lattice within the Fe_3Sn_2 shows giant spin-orbit tunability[4,5] and the long sorted magnetic Weyl semimetals were identified in kagome $Co_3Sn_2S_2$.[6−8] Recently, the newly discovered quasi-two-dimensional kagome materials, which are KV_3Sb_5, RbV_3Sb_5, and CsV_3Sb_5, open a new avenue for connecting the superconductivity with kagome physics,[3,9−19] escalating the curiosity of physics community to uncover even more unconventional quantum phenomena from the kagome lattice.

Unfortunately, finding the desired kagome materials is a challenging task. For example, only three CsV_3Sb_5-like superconductive kagome materials (as mentioned above) have been experimentally synthesized at the time of writing, limiting the investigation of kagome superconductivity to a fairly small compound space. Hence, the development of quantum physics hinges pretty much on finding a viable material system with low dimensionality as well as various symmetry-breaking instabilities (such as superconductivity).

In order to search for promising kagome materials, this work systematically evaluates 1386 structures of kagome materials with the stoichiometry of AM_3X_5 (A for alkali elements, M for transition metals, and X for anionic elements from Ⅲ A, Ⅳ A, V A), which is derived from the CsV_3Sb_5 (space group *P6/mmm*). Employing the high-throughput calculations at the density functional theory level as well as the atomly.net[20] materials database, the optimized structure, thermodynamic stability (energy above hull < 5 meV/atom), and electronic structures are calculated, and, in the end, 28 promising candidates pop up from the screening process, including the CsV_3Sb_5, RbV_3Sb_5, and KV_3Sb_5, i.e., the three known compounds that have been experimentally made according to existing literature, validating the reliability of our calculations. Among the 25 new compounds, it is found that the non-magnetic can be grouped into five non-magnetic categories based on their electronic structures. There are also a handful of magnetic kagome materials that fall out of the screening, and they are likely the feasible compounds to materialize the spin-related quantum phenomena in kagome lattice. This work charts a synthesizability "treasure hunt map", from the theory-

†Y. Jiang and Z. Yu contributed equally to this work.
*Corresponding authors. Email: smeng@iphy.ac.cn; jiangkun@iphy.ac.cn; mliu@iphy.ac.cn

and data-driven approach, for quantum material community to discover the viable kagome materials.

Methodology. The theoretical calculations are performed at density functional theory (DFT)[21] level in a high-throughput mode to evaluate the properties of AM_3X_5 kagome systems. The DFT calculations are carried out using the Vienna *ab initio* software package (VASP)[22,23] with the projector augmented-wave[24,25] method to describe the nucleus–electron interactions and the generalized gradient approximation (GGA) within the Perdew–Burke–Ernzerhof (PBE)[26] framework to describe the exchange-correlation in-between electrons. The plane-wave cutoff energy is 520 eV, the energy convergence criterion is 5×10^{-6} eV, and the K-points grid density of 100 k-points/Å^{-3} is adopted for all the calculations. All the calculations are conducted in a high-throughput mode by employing the standardized parameters to ensure that the calculation results (especially the formation energy) are mutually comparable to each other.

Results. In order to search for CsV_3Sb_5-like compounds that are highly synthesizable, 1386 structures are generated by employing the CsV_3Sb_5 (space group *P6/mmm*) as the structural template, then an element substitution process [as shown in Fig. 1(a)] is performed by replacing Cs site with (H, Li, Na, K, Rb, Cs), substituting V site with (Ti, Zr, Hf, V, Nb, Ta, Cr, Mo, W, Mn, Tc, Re, Fe, Ru, Os, Co, Rh, Ir, Ni, Pd, Pt), and replacing Sb site with (Si, Ge, Sn, Pb, P, As, Sb, Bi, S, Se, Te), totaling 1386 structures (including the CsV_3Sb_5). The purpose of the procedure is to create a large pool of candidate materials for future calculation and screening.

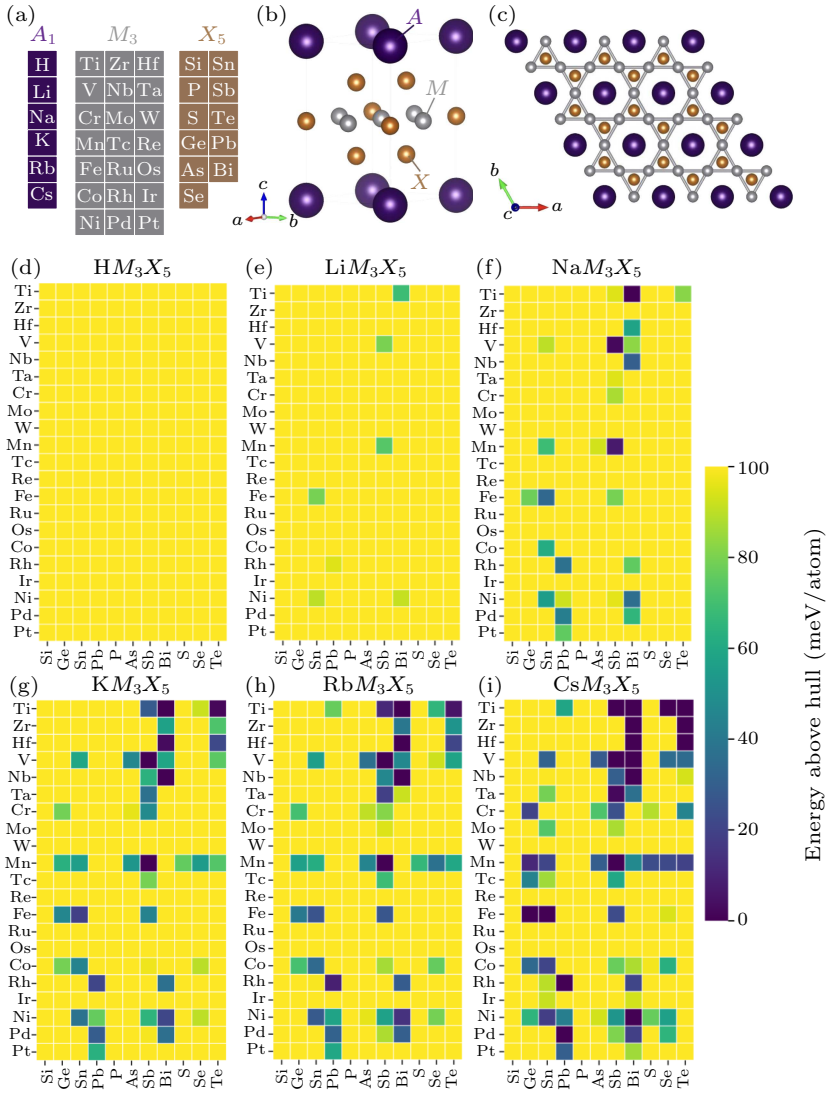

Fig. 1. The structure and thermodynamic stability of the CsV_3Sb_5-like kagome compounds. (a)–(c) The structure and the schematic of the element substitution strategy for generating CsV_3Sb_5-like compounds, and the transition metal forms the kagome lattice in the structure. (d)–(i) The thermodynamic stability (represented quantitatively as $E_{\rm hull}$) for 1386 compounds in a heat map plotting mode. Each box shows an AM_3X_5 compound, and the darker the color, the more stable the compound is. Compounds with $E_{\rm hull}$ greater than 100 meV/atom are plotted in yellow.

Then the high-throughput calculations are performed with an in-house workflow for structure optimization, high precision static calculation and electronic structure (density of states and energy bands) calculation. The structure optimization process relaxes the cell volume and the position of each atom in the structure to yield the equilibrium ground state of the given structure at 0 K, then the total energy obtained from the static calculation is used to justify the thermodynamic stability of the compound. In practice, the compound is put together with all available phases from the same chemical system to evaluate the phase competition. In order to get as many compounds as available from the same chemical system, we first query all the compounds from the atomly.net,[20] which is an open-access materials database, to get all the relevant data. Then the data is plugged into the PhaseDiagram module[27] from the pymatgen[28] to generate the phase diagrams for each chemical system to obtain the energy above hull ($E_{\rm hull}$) of each AM_3X_5 kagome material. Basically, the formation energy means the energy released or consumed when one unit of a substance is created under standard conditions from its pure elements.[27,29] The compounds with smaller formation energy (negative value for energy release) are thermodynamically more stable. The most stable compounds open a formation energy convex hull to describe the lower boundary of the formation energies, and $E_{\rm hull}$ simply denotes the distance between formation energy of a compound to the energy convex hull. In short, $E_{\rm hull}$ of a compound quantitatively measures the driving force (in units of energy) to decompose the compound to the most stable phases. The comprehensive concept of $E_{\rm hull}$ can be found in Refs. [30–32] and in Fig. S1 of the Supplementary Material. In general, smaller $E_{\rm hull}$ represents better stability. Normally, nonmetallic compounds with $E_{\rm hull} < 50$ meV/atom or alloys/metals with $E_{\rm hull} < 10$ meV/atom are likely to exist in real world.

Figures 1(d)–1(i) show the $E_{\rm hull}$ of AM_3X_5 compounds from our calculations. It can be observed that all the HM_3X_5 and LiM_3X_5 compounds are thermodynamically unstable as their $E_{\rm hull}$ values are all larger than 60 meV/atom. In the rest chemical space, $E_{\rm hull}$ values of 28 compounds are under 5 meV/atom (Table 1), $E_{\rm hull}$ values of 38 compounds are less than 20 meV/atom (see Table S1 for complete list), and $E_{\rm hull}$ values of 90 compounds are smaller than 50 meV/atom (see Table S2 for complete list).

Table 1. List of 28 compounds with good thermodynamic stability ($E_{\rm hull} < 5$ meV/atom). The compound formula, ID in the database, $E_{\rm hull}$ values, lattice parameters and the magnetization are provided. FM: ferromagnetic.

Formula	ID (atomly.net)	$E_{\rm hull}$ (meV/atom)	a (Å)	c (Å)	Magnetization ($\mu_{\rm B}$/formula)
$NaTi_3Bi_5$	1000299281	0	5.78	9.18	
NaV_3Sb_5	1000299291	2	5.46	8.91	
KTi_3Bi_5	1000299512	0	5.79	9.72	
KV_3Sb_5	1000299522	0	5.48	9.37	
KMn_3Sb_5	1000299544	0	5.43	9.26	FM ($\mu = 7.75$)
KNb_3Bi_5	1000299600	0	5.89	9.59	
KHf_3Bi_5	1000299666	3	6.08	9.45	
$RbTi_3Bi_5$	1000299743	0	5.79	9.89	
RbV_3Sb_5	1000299753	0	5.50	9.38	
$RbMn_3Sb_5$	1000299775	0	5.44	9.44	FM ($\mu = 7.73$)
$RbNb_3Bi_5$	1000299831	0	5.89	9.71	
$RbHf_3Bi_5$	1000299897	0	6.08	9.59	
$CsTi_3Sb_5$	1000299973	0	5.68	9.81	
$CsTi_3Bi_5$	1000299974	0	5.83	9.92	
$CsTi_3Te_5$	1000299981	0	6.10	8.91	
CsV_3Sb_5	1000299984	0	5.49	9.89	
CsV_3Bi_5	1000299985	0	5.64	10.15	
$CsMn_3Sb_5$	1000300006	0	5.44	9.69	FM ($\mu = 7.70$)
$CsFe_3Ge_5$	1000300020	0	4.89	9.73	FM ($\mu = 4.99$)
$CsFe_3Sn_5$	1000300021	0	5.26	10.53	FM ($\mu = 6.50$)
$CsZr_3Bi_5$	1000300051	0	6.11	10.09	
$CsZr_3Te_5$	1000300058	0	6.41	9.07	
$CsNb_3Bi_5$	1000300062	0	5.91	9.87	
$CsRh_3Pb_5$	1000300110	0	5.71	9.74	
$CsPd_3Pb_5$	1000300121	0	5.81	9.61	
$CsHf_3Bi_5$	1000300128	0	6.09	10.05	
$CsHf_3Te_5$	1000300135	0	6.35	8.76	
$CsTa_3Sb_5$	1000300138	2	5.81	9.60	

Table 1 presents the full list of the 28 compounds that fall out of the $E_{\rm hull} < 5\,{\rm meV/atom}$ screening. It is found that three known compounds, which are CsV_3Sb_5, RbV_3Sb_5, and KV_3Sb_5, show up on the list, suggesting that the screening treatment is fairly effective and accurate. It can be observed that the stable AM_3X_5 structures can be found in AV_3Sb_5 ($A =$ Na, K, Rb, Cs), ANb_3Bi_5 ($A =$ K, Rb, Cs), ATi_3Bi_5 ($A =$ Na, K, Rb, Cs), AMn_3Sb_5 ($A =$ K, Rb, Cs), AHf_3Bi_5 ($A =$ K, Rb, Cs), $CsTi_3Te_5$, $CsTi_3Sb_5$, CsV_3Bi_5, $CsFe_3Ge_5$, $CsFe_3Sn_5$, $CsZr_3Bi_5$, $CsZr_3Te_5$, $CsHf_3Te_5$, $CsTa_3Sb_5$, $CsRh_3Pb_5$, and $CsPd_3Pb_5$. It is also found that the stability of AM_3X_5 decreases sequentially when A site is occupied by H, Li, Na, K, Rb, Cs, and the later transition metal on M site is unlikely to yield stable AM_3X_5. Cs on A site can stabilize the structure as 16 out of 28 stable compounds in Table 1 are Cs-containing compounds, and it seems that the stability of AM_3X_5 is largely determined by the M–X layer as V–Sb, Nb–Bi, Ti–Bi, Mn–Sb, and Hf–Bi combinations are more stable. Overall, the viable AM_3X_5 kagome lattices are limited to a small phase space based on our screening, and Fig. 1 and Table 1 chart a likelihood 'map' for discovering the viable CsV_3Sb_5-like compounds.

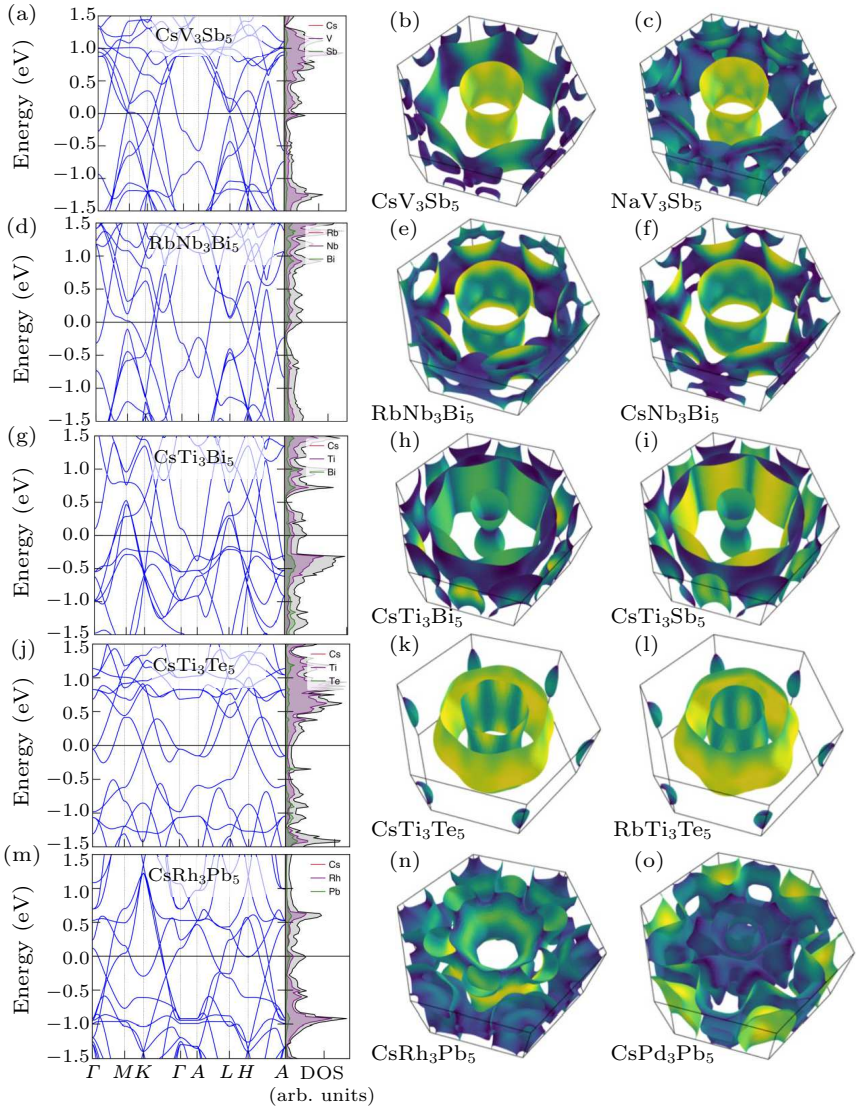

Fig. 2. Electronic structures of selected non-magnetic compounds with $E_{\rm hull} < 5\,{\rm meV/atom}$. The compounds are categorized into five dedicated groups, as (a)–(c), (d)–(f), (g)–(i), (j)–(l), (m)–(o), according to their band structures, density of states and Fermi surfaces. Compounds in the same group have very similar electronic structures.

Since the electronic structures, especially the flat-band, Dirac-point (DP), and van Hove singularity (VHS), are fairly important properties of kagome lattice, the electronic structures of all the CsV_3Sb_5-like compounds (1386 of them in total) are calculated at GGA-PBE level without considering the spin orbital

coupling. It is found that the AM_3X_5 can be classified into five non-magnetic groups and three magnetic groups according to their energy bands and Fermi surface. Figure 2 shows the representative compounds of the five non-magnetic types and their electronic structures. The CsV_3Sb_5 is the most known type, and the DP is below the Fermi surface and the VHS is close to or at the Fermi surface. Other than AV_3Sb_5 ($A=$ Na, K, Rb, Cs), CsV_3Bi_5 is also in this group. For the $RbNb_3Bi_5$-type, the DP is below the Fermi surface, the VHS is close to or at the Fermi surface, but the bands, except the VHS band, at the M point open up a gap. KNb_3Bi_5, $RbNb_3Bi_5$, $CsNb_3Bi_5$, and $CsTa_3Sb_5$ belong to this type of compound. The $CsTi_3Bi_5$-type shots up both the DP and VHS as those compounds have less valence electrons than that of the CsV_3Sb_5 type, hence it can be regarded as the hole-doped CsV_3Sb_5-type and the Fermi surface is moved downward to some extent. ATi_3Bi_5 ($A=$ Na, K, Rb, Cs), AHf_3Bi_5 ($A=$ K, Rb, Cs), $CsTi_3Sb_5$, and $CsZr_3Bi_5$ can be classified into this electronic structure type. In the $CsTi_3Te_5$-type compounds, the VHS band is vanished and the DP is located fairly close to the Fermi surface, forming a simple Fermi surface in reciprocal space as there are fewer bands around. $CsTi_3Te_5$, $CsZr_3Te_5$, and $CsHf_3Te_5$ are the similar type of compounds. The $CsRh_3Pb_5$-type compounds are more three-dimensional losing the typical feature of two-dimensional Kagome lattice. $CsRh_3Pb_5$ still has the VHS band near the Fermi surface but lacks the DP bands, and $CsRh_3Pb_5$, $CsPd_3Pb_5$ are this type of compounds.

For the Mn- and Fe-containing AM_3X_5 structures, the compounds are spin-polarized and show ferromagnetism as shown in Fig. 3. There are only a few of compounds in this type, which are AMn_3Sb_5 ($A=$ K, Rb, Cs), $CsFe_3X_5$ ($X=$ Ge, Sn). It is fairly special that the kagome sites in those compounds are spin-polarized, making them the viable material systems to materialize the spin-related phenomenon.[1,2,33,34] At the collinear level of treatment for the system, it is observed that the Mn or Fe kagome sites hold the prominent amount of magnetic moment, e.g., the magnetic moment of Mn sites in $CsMn_3Sb_5$ is around 2.5–2.7 μ_B/atom while the total magnetic moment of the compound is around 7.5–8.0μ_B per formula. Because of the non-degenerated orbitals caused by the spin-polarization, the Fermi surface in the reciprocal space manifests much more complicated structures, and the DP and VHS also split into two sets. Hence, our work hints that it is likely to have spin-polarized CsV_3Sb_5-like kagome materials, and a drilled-down study is worth conducting.

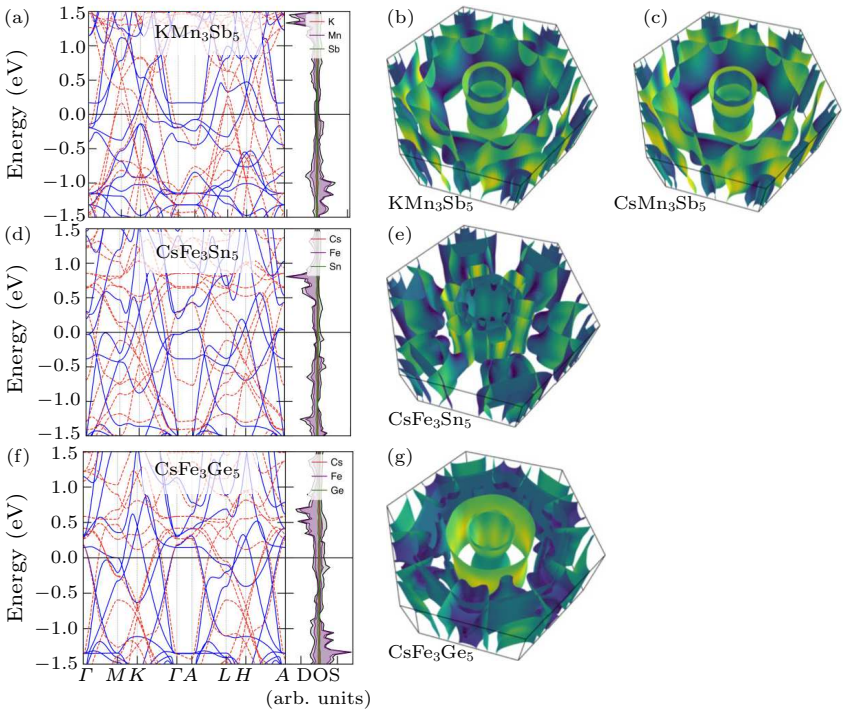

Fig. 3. Electronic structures of magnetic compounds with $E_{\rm hull} < 5$ meV/atom. (a)–(c), (d) and (e), (f) and (g) are band structures, density of states and Fermi surfaces of representative compounds.

Discussion. Based on our screening, we are offering the community a ranked list for discovering new compounds that share the same crystal structure with CsV_3Sb_5. We indeed obtain a compound list of CsV_3Sb_5-like compounds, and provide a systematic evaluation of formation energy landscape for them. Considering that the formation energy of the alloy is generally small compared to that of the ionic and covalent compounds, and the formation energy between the compounds is still relatively close to each other, therefore, it is generally difficult to synthesize the intermetallic phases even when they are predicted to be stable.

The data we utilized to generate the phase diagram cover a very large compound space as most ICSD[35] and materials project[36] structures are included. What's more, we have generated and calculated $\sim 100k$ new structures by replacing the element species. The large compound space can ensure the accurate gauging of the E_{hull} of compounds, but there is still a small chance to overlook the most stable compounds that can stretch the hull to even lower energies. In such a case, the E_{hull} of most compounds can be lifted up a little, hence the value of the E_{hull} may increase a little when the database grows larger.

Tables 1, S1, and S2 serve as synthesis guides for exploring the CsV_3Sb_5-like compounds. If the pure phases of those predicted compounds are hard to make, it will be highly possible that the doped compounds can be experimentally realized employing the knowledge from Fig. 1. For example, hole- or electron-doping to CsV_3Sb_5 compounds could probably be experimentally realized by replacing a small amount of the V with Ti or Ni,[37,38] and substituting small amount of the V with Mn or Fe can possibly introduce magnetism into these material systems. Figures 2 and 3 provide guides on how the electronic structures can be tuned when mixing the metal elements. Although the present main text shows the 28 most stable compounds, those compounds in Table S1 also have good-to-moderate stability, and are worth looking at. For example, the CsV_6Sb_6, which has an E_{hull} of ~ 12 meV/atom based on our calculation, has been experimentally made.[39–41]

The electronic structures of all the 28 compounds in Table 1 can be found in the Supplementary Material (Fig. S2). The calculated data for all the 1386 compounds is open-accessible from atomly.net[20] (for people who has a user account).

In summary, this work widens the knowledge of the CsV_3Sb_5 family through high-throughput calculation and systematic evaluation. Via the element replacement, a large chemical space of the CsV_3Sb_5-like materials (1386 in total) is calculated at the GGA-PBE level employing the DFT. The systematic evaluation tells us that there are at least 28 compounds having excellent thermodynamic stability, and therefore they look forward to further experimental confirmation. The electronic structures of those materials add possibilities for rational band structure engineering of kagome quantum materials. It is our hope that useful new kagome materials can be experimentally discovered for quantum physics community based on our prediction.

Acknowledgements. We would acknowledge the financial support from the Chinese Academy of Sciences (Grant Nos. ZDBS-LY-SLH007, XDB33020000, and CAS-WX2021PY-0102), and the National Natural Science Foundation of China (Grant No. 12174428). The computational resource is provided by the Platform for Data-Driven Computational Materials Discovery of the Songshan Lake Laboratory. We also thank Youguo Shi for discussion.

References

[1] Zhou Y, Kanoda K and Ng T K 2017 *Rev. Mod. Phys.* **89** 025003
[2] Balents L 2010 *Nature* **464** 199
[3] Jiang K, Wu T, Yin J X *et al.* 2021 arXiv:2109.10809 [cond-mat.supr-con]
[4] Yin J X, Zhang S S, Li H *et al.* 2018 *Nature* **562** 91
[5] Ye L, Kang M, Liu J *et al.* 2018 *Nature* **555** 638
[6] Liu E, Sun Y, Kumar N *et al.* 2018 *Nat. Phys.* **14** 1125
[7] Liu D F, Liang A J, Liu E K *et al.* 2019 *Science* **365** 1282
[8] Morali N, Batabyal R, Nag P K, Liu E, Xu Q, Sun Y, Yan B, Felser C, Avraham N and Beidenkopf H 2019 *Science* **365** 1286
[9] Ortiz B R, Teicher S M L, Hu Y *et al.* 2020 *Phys. Rev. Lett.* **125** 247002
[10] Ortiz B R, Gomes L C, Morey J R *et al.* 2019 *Phys. Rev. Mater.* **3** 094407
[11] Ortiz B R, Sarte P M, Kenney E M, Graf M J, Teicher S M L, Seshadri R and Wilson S D 2021 *Phys. Rev. Mater.* **5** 034801
[12] Yin Q, Tu Z, Gong C, Fu Y, Yan S and Lei H 2021 *Chin. Phys. Lett.* **38** 037403
[13] Mielke C, Das D, Yin J X, Liu H, Gupta R, Jiang Y X, Medarde M, Wu X, Lei H C, Chang J, Dai P, Si Q, Miao H, Thomale R, Neupert T, Shi Y, Khasanov R, Hasan M Z, Luetkens H and Guguchia Z 2022 *Nature* **602** 245
[14] Yu L, Wang C, Zhang Y *et al.* 2021 arXiv:2107.10714 [cond-mat.supr-con]
[15] Chen H, Yang H, Hu B *et al.* 2021 *Nature* **599** 222
[16] Nie L, Sun K, Ma W, Song D, Zheng L, Liang Z, Wu P, Yu F, Li J, Shan M, Zhao D, Li S, Kang B, Wu Z, Zhou Y, Liu K, Xiang Z, Ying J, Wang Z, Wu T and Chen X 2022 *Nature* (in press)
[17] Mu C, Yin Q, Tu Z, Gong C, Lei H, Li Z and Luo J 2021 *Chin. Phys. Lett.* **38** 077402
[18] Ni S, Ma S, Zhang Y *et al.* 2021 *Chin. Phys. Lett.* **38** 057403
[19] Chen X, Zhan X, Wang X, Deng J, Liu X B, Chen X, Guo J G and Chen X 2021 *Chin. Phys. Lett.* **38** 057402
[20] *Atomly* https://atomly.net/
[21] Kohn W and Sham L J 1965 *Phys. Rev.* **140** A1133
[22] Kresse G and Furthmüller J 1996 *Comput. Mater. Sci.* **6** 15
[23] Kresse G and Furthmüller J 1996 *Phys. Rev. B* **54** 11169
[24] Blöchl P E 1994 *Phys. Rev. B* **50** 17953
[25] Kresse G and Joubert D 1999 *Phys. Rev. B* **59** 1758
[26] Perdew J P, Burke K and Ernzerhof M 1996 *Phys. Rev.*

Lett. **77** 3865
[27] Ong S P, Wang L, Kang B and Ceder G 2008 *Chem. Mater.* **20** 1798
[28] Ong S P, Richards W D, Jain A, Hautier G, Kocher M, Cholia S, Gunter D, Chevrier V L, Persson K A and Ceder G 2013 *Comput. Mater. Sci.* **68** 314
[29] Liu M, Rong Z, Malik R, Canepa P, Jain A, Ceder G and Persson K A 2015 *Energy & Environ. Sci.* **8** 964
[30] Ong S P, Jain A, Hautier G, Kang B and Ceder G 2010 *Electrochem. Commun.* **12** 427
[31] Sun W, Dacek S T, Ong S P, Hautier G, Jain A, Richards W D, Gamst A C, Persson K A and Ceder G 2016 *Sci. Adv.* **2** e1600225
[32] Barber C B, Dobkin D P and Huhdanpaa H 1996 *ACM Trans. Math. Softw.* **22** 469
[33] Villain J, Bidaux R, Carton J P and Conte R 1980 *J. Phys. France* **41** 1263
[34] Ran Y, Hermele M, Lee P A and Wen X G 2007 *Phys. Rev. Lett.* **98** 117205
[35] *ICSD* https://icsd.products.fiz-karlsruhe.de/
[36] Jain A, Ong S P, Hautier G, Chen W, Richards W D, Dacek S, Cholia S, Gunter D, Skinner D, Ceder G and Persson K A 2013 *APL Mater.* **1** 11002
[37] Yang H, Zhang Y, Huang Z *et al.* 2021 arXiv:2110.11228 [cond-mat.supr-con]
[38] Oey Y M, Ortiz B R, Kaboudvand F *et al.* 2021 arXiv:2110.10912 [cond-mat.supr-con]
[39] Shi M, Yu F, Yang Y, Meng F *et al.* 2021 arXiv:2110.09782 [cond-mat.supr-con]
[40] Yin Q, Tu Z, Gong C, Tian S and Lei H 2021 *Chin. Phys. Lett.* **38** 127401
[41] Yang Y, Fan W, Zhang Q *et al.* 2021 *Chin. Phys. Lett.* **38** 127102

Supplementary Material for

Screening Promising CsV_3Sb_5-Like Kagome Materials from Systematic First-Principles Evaluation

Yutao Jiang(姜昱韬)[1,2], Ze Yu(喻泽)[1,2], Yuxin Wang(王郁欣)[1,2], Tenglong Lu(芦腾龙)[1,2], Sheng Meng(孟胜)[1,2,3 *], Kun Jiang(蒋坤)[1,3 *], and Miao Liu(刘淼)[1,3,4 *]

[1]Beijing National Laboratory for Condensed Matter Physics, Institute of Physics, Chinese Academy of Sciences, Beijing, 100190, China

[2]School of Physical Sciences, University of Chinese Academy of Sciences, Beijing 100190, China

[3]Songshan Lake Materials Laboratory, Dongguan, Guangdong, 523808, China

[4]Center of Materials Science and Optoelectronics Engineering, University of Chinese Academy of Sciences, Beijing, 100049, P. R. China

*Corresponding author: smeng@iphy.ac.cn, jiangkun@iphy.ac.cn, mliu@iphy.ac.cn.

Figure S1. Schematic demonstration of energy above hull (E_{hull}) with an example of A-B binary system.

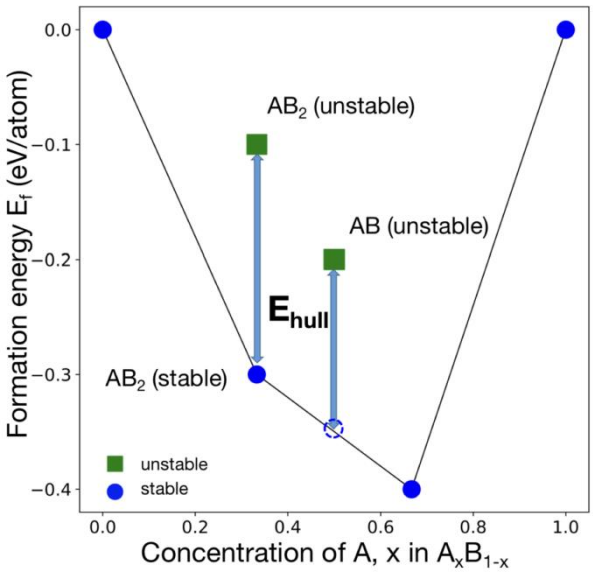

Figure S1 demonstrates the concept of energy above hull (E_{hull}) with an example of A-B binary chemical system. Different phases of this binary system are plotted. The blue dots represent thermodynamically stable phases and the green squares represent unstable phases. The linking lines of stable phases form the convex hull of this chemical system. The E_{hull} of a phase is defined as the energy difference between its formation energy and the energy of convex hull at its composition. It should be noted that when no stable phase could be found at certain composition (like AB in Fig. S1), E_{hull} of a phase actually represents the energy difference of its formation energy with possible linear combination of neighboring stable phases (marked with a dashed blue circle in Fig. S1). In this case, E_{hull} measures the tendency for possible decomposition of a phase into the neighboring stable phases.

Figure S2 is the electronic structures of all the 28 compounds with E_{hull} less than 5 meV/atom. Table S1 is property list of compounds with $5 < E_{hull} < 20$ meV/atom, and table S2 is property list of compounds with $20 < E_{hull} < 50$ meV/atom.

Figure S2. Electronic structures of 28 compounds with E_{hull} < 5 meV/atom.

NaTi3Bi5
1000299281

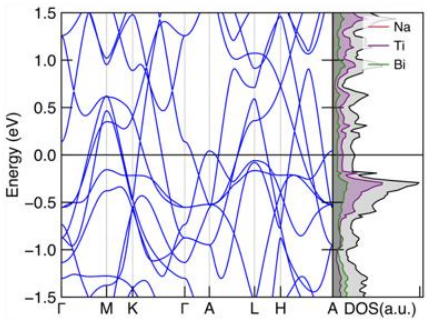

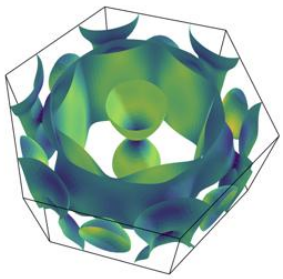

NaV3Sb5
1000299291

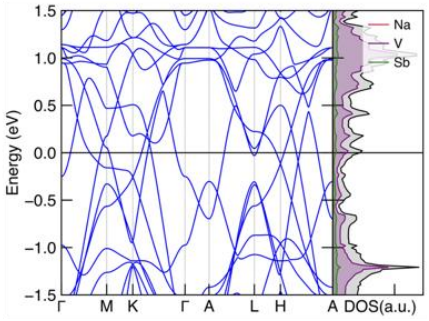

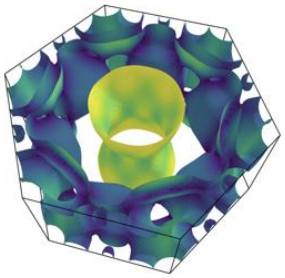

KTi3Bi5
1000299512

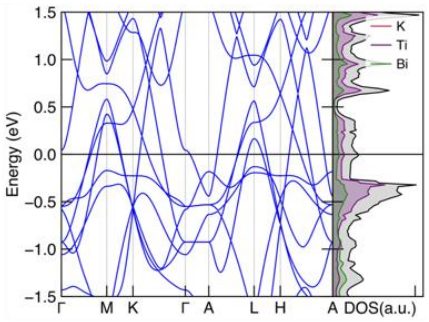

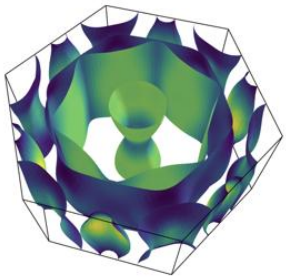

KV3Sb5
1000299522

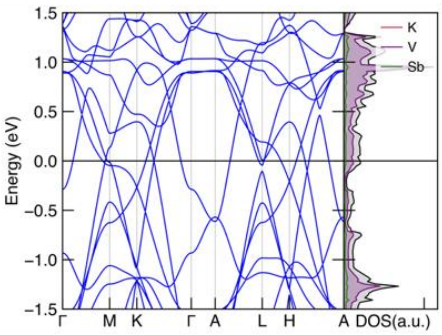

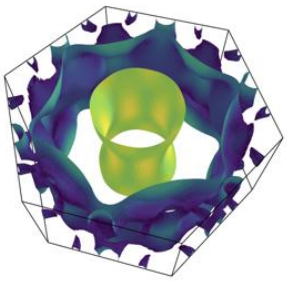

RbMn3Sb5
1000299775

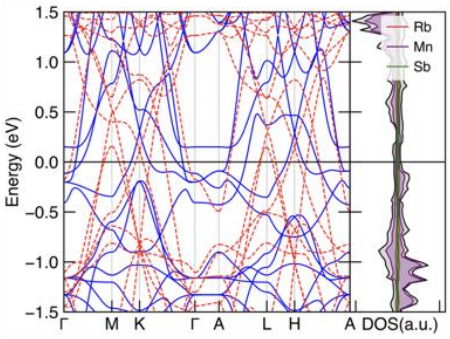

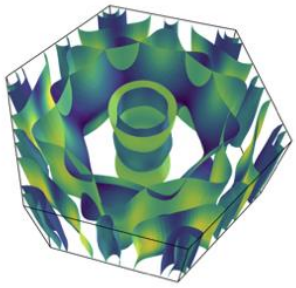

RbNb3Bi5
1000299831

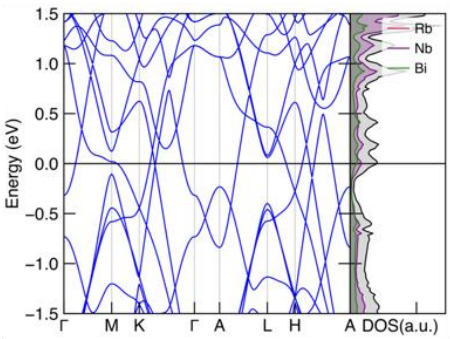

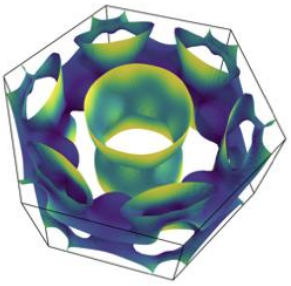

RbHf3Bi5
1000299897

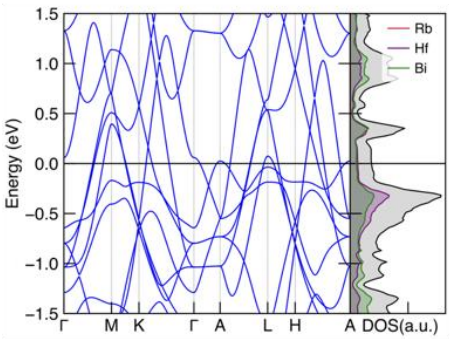

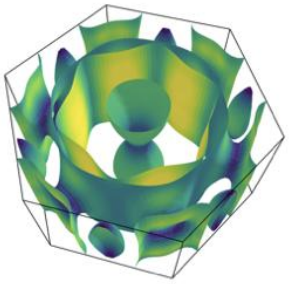

CsTi3Sb5
1000299973

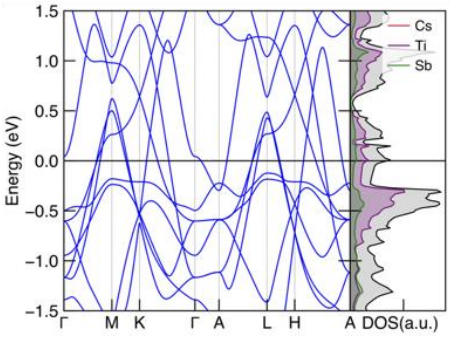

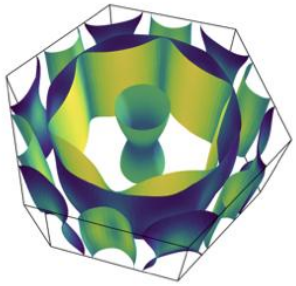

CsTi3Bi5
1000299974

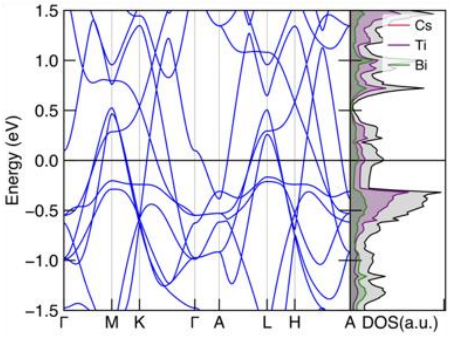

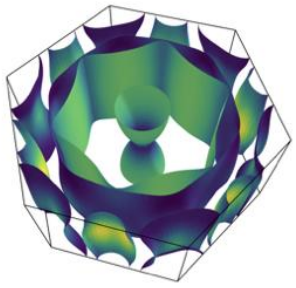

KMn3Sb5
1000299544

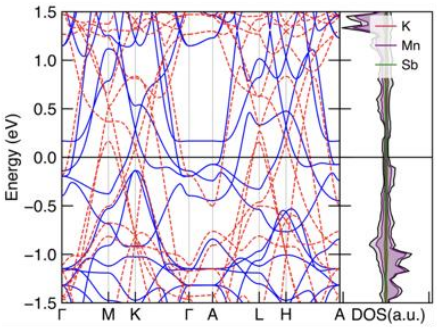

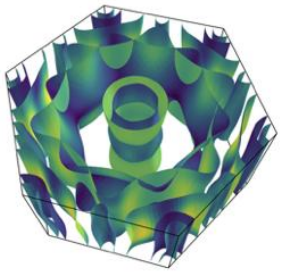

KNb3Bi5
1000299600

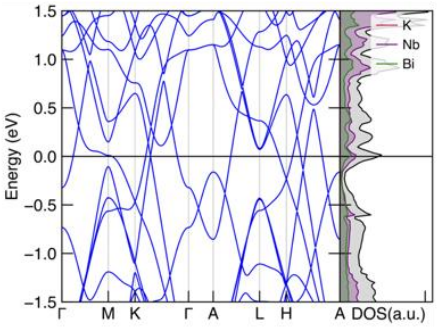

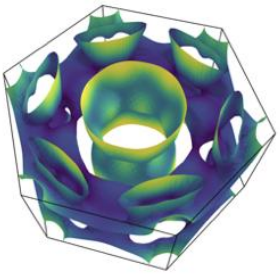

KHf3Bi5
1000299666

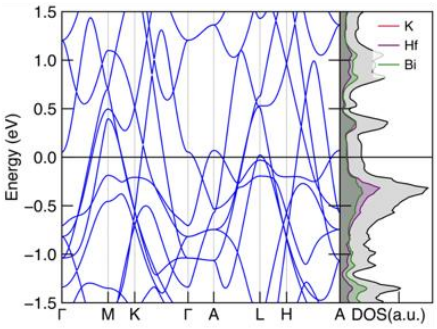

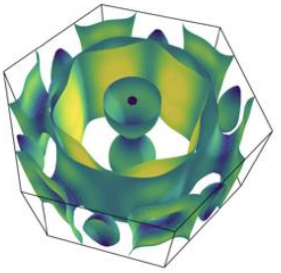

RbTi3Bi5
1000299743

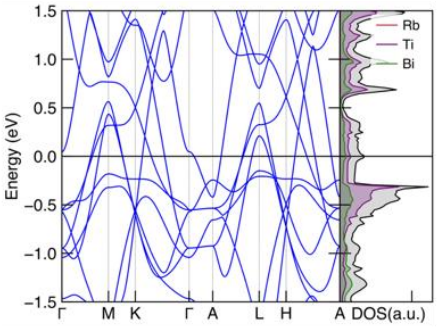

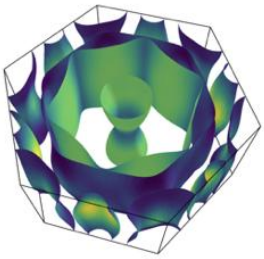

RbV3Sb5
1000299753

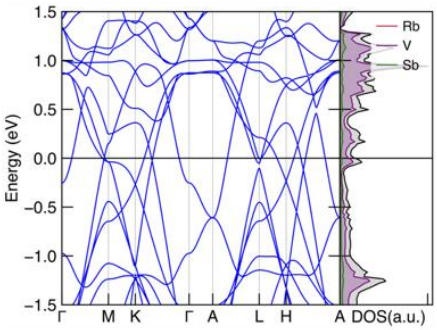

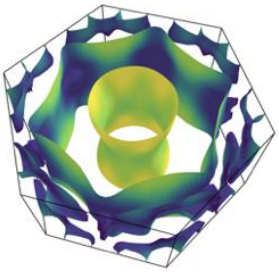

CsTi3Te5
1000299981

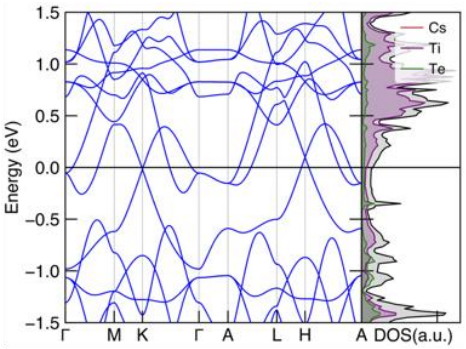

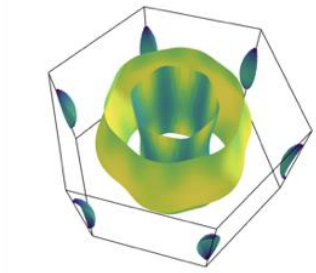

CsV3Sb5
1000299984

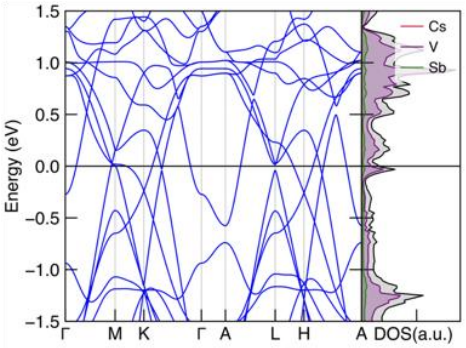

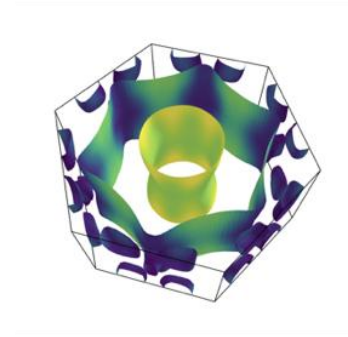

CsV3Bi5
1000299985

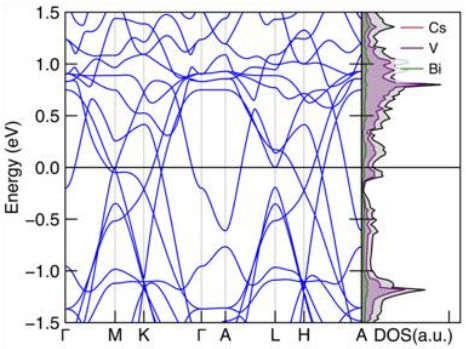

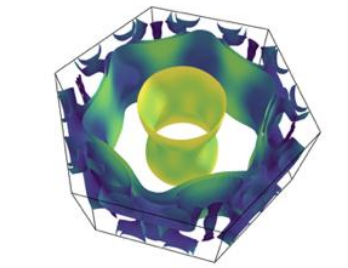

CsMn3Sb5
1000300006

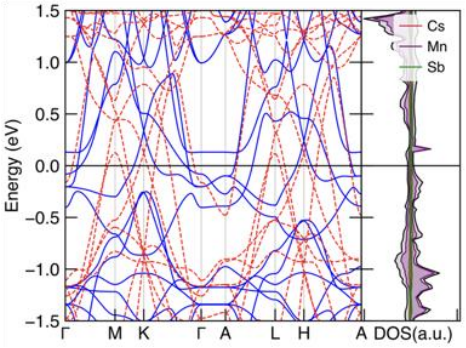

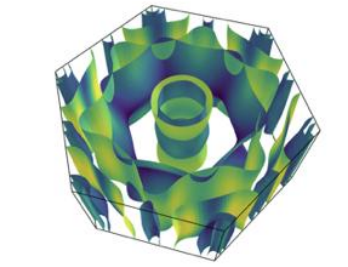

CsFe3Ge5
1000300020

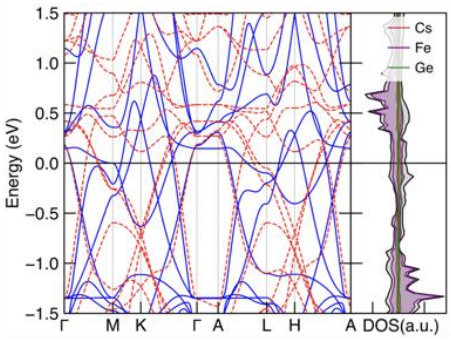

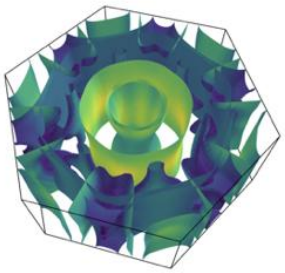

CsFe3Sn5
1000300021

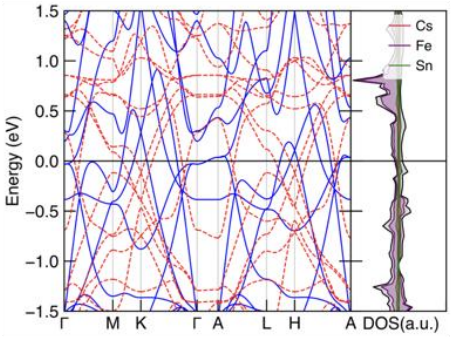

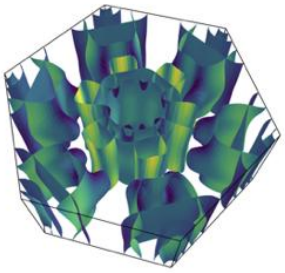

CsTa3Sb5
1000300138

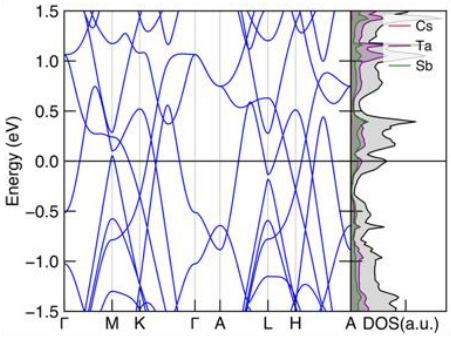

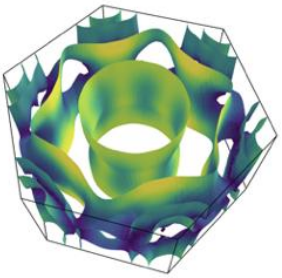

CsZr3Bi5
1000300051

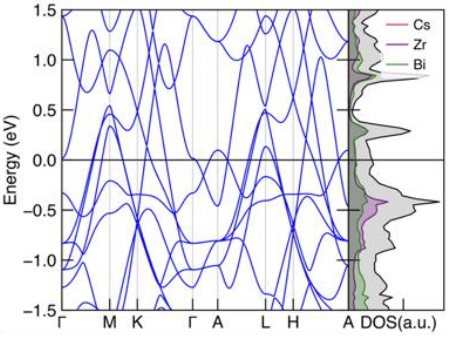

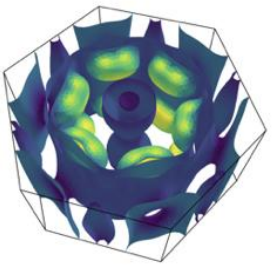

CsZr3Te5
1000300058

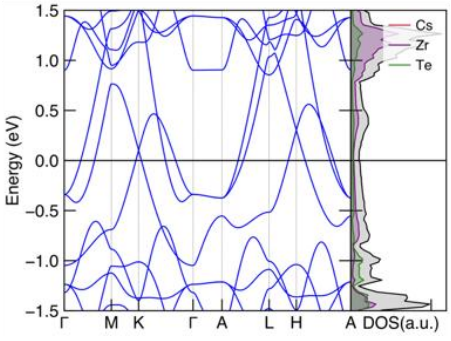

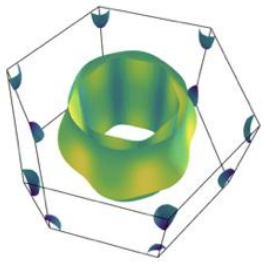

CsNb3Bi5
1000300062

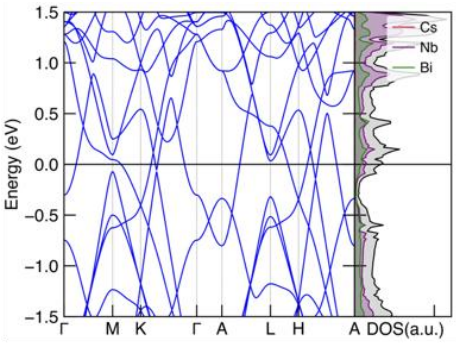

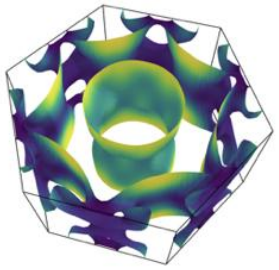

CsRh3Pb5
1000300110

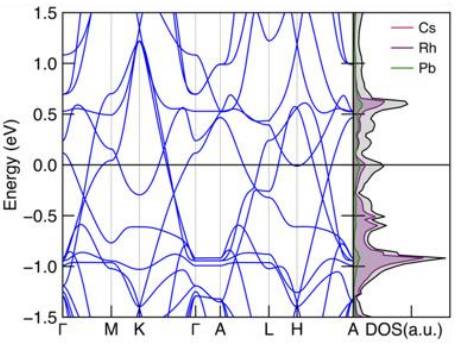

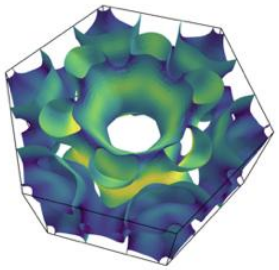

CsPd3Pb5
1000300121

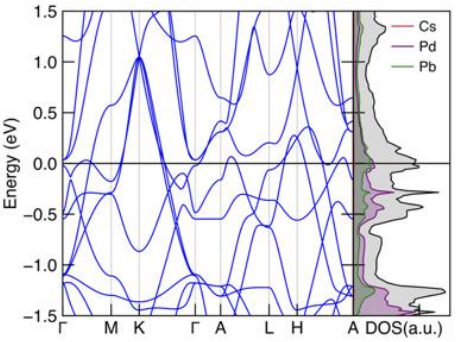

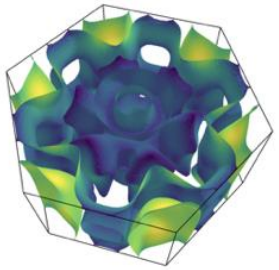

CsHf3Bi5
1000300128

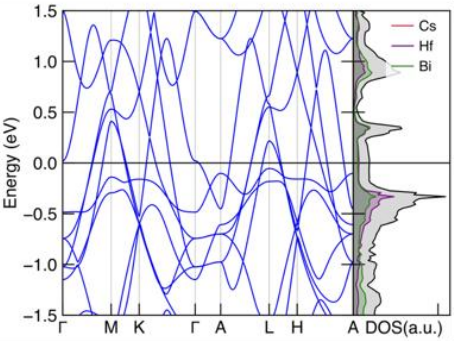

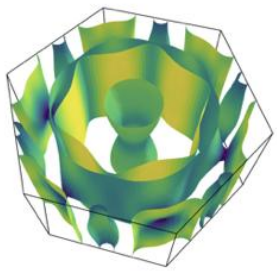

CsHf3Te5
1000300135

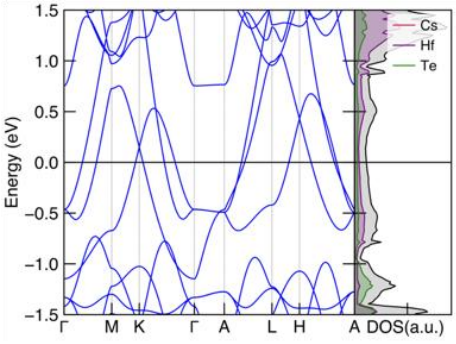

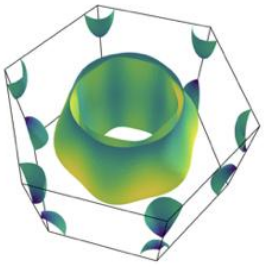

Table S1. Property list of 11 compounds with 5 < E_{hull} < 20 (meV/atom)

formula	id(atomly.net)	Ehull(meV/atom)	a(Å)	c(Å)	magnetization
NaMn3Sb5	1000299313	7	5.40	8.79	FM(μ =7.68)
KFe3Sn5	1000299559	19	5.24	9.53	FM(μ =6.51)
RbTi3Sb5	1000299742	11	5.66	9.63	
RbTi3Te5	1000299750	5	6.09	8.54	
RbRh3Pb5	1000299879	9	5.71	9.23	
RbTa3Sb5	1000299907	19	5.79	9.58	
CsMn3Ge5	1000300009	11	4.99	9.42	FM(μ =4.21)
CsMn3Te5	1000300014	20	6.15	8.30	FM(μ =9.48)
CsNi3Sn5	1000300043	18	5.21	10.21	
CsBi5Pd3	1000300117	19	5.88	9.67	

Table S2. Property list of 52 compounds with 20 < E_{hull} < 50 meV/atom

formula	id(atomly.net)	Ehull(meV/atom)	a(Å)	c(Å)	magnetization
NaFe3Sn5	1000299328	34	5.23	8.75	FM(μ =6.24)
NaNb3Bi5	1000299369	30	5.87	9.16	
NaRh3Pb5	1000299417	37	5.70	8.23	
NaPd3Pb5	1000299428	42	5.75	8.35	
KTi3Sb5	1000299511	28	5.66	9.39	
KTi3Te5	1000299519	24	6.07	8.48	
KV3As5	1000299521	46	5.20	8.66	
KFe3Sb5	1000299555	44	5.40	9.20	FM(μ =6.56)
KFe3Ge5	1000299558	46	4.87	9.01	FM(μ =4.90)
KCo3Sn5	1000299570	45	5.24	9.28	
KNi3Sn5	1000299581	38	5.20	9.33	
KBi5Rh3	1000299644	36	5.81	9.21	
KRh3Pb5	1000299648	21	5.70	9.02	
KBi5Pd3	1000299655	36	5.87	8.87	
KPd3Pb5	1000299659	29	5.82	8.53	
KHf3Te5	1000299673	40	6.33	8.57	
KTa3Sb5	1000299676	37	5.79	9.31	
RbV3As5	1000299752	37	5.22	8.71	
RbV3Bi5	1000299754	47	5.63	9.69	
RbMn3As5	1000299774	45	5.18	8.73	FM(μ =5.84)
RbMn3Se5	1000299782	37	5.97	7.40	FM(μ =10.36)
RbFe3Sb5	1000299786	30	5.40	9.42	FM(μ =6.52)
RbFe3Ge5	1000299789	40	4.90	9.17	FM(μ =5.03)
RbFe3Sn5	1000299790	26	5.24	9.88	FM(μ =6.51)

RbCo3Sn5	1000299801	34	5.25	9.55	
RbNi3Sn5	1000299812	28	5.21	9.78	
RbZr3Bi5	1000299820	40	6.12	9.63	
RbNb3Sb5	1000299830	46	5.80	9.61	
RbBi5Rh3	1000299875	29	5.83	9.31	
RbBi5Pd3	1000299886	30	5.87	9.39	
RbPd3Pb5	1000299890	31	5.79	9.34	
RbHf3Te5	1000299904	21	6.34	8.62	
CsV3As5	1000299983	28	5.23	8.97	
CsV3Sn5	1000299988	31	5.40	10.01	
CsV3Se5	1000299991	35	5.68	7.93	FM(μ =2.98)
CsV3Te5	1000299992	35	6.02	8.71	FM(μ =3.76)
CsCr3Sb5	1000299995	47	5.50	9.70	FM(μ =4.54)
CsCr3Ge5	1000299998	20	4.95	9.61	
CsCr3Te5	1000300003	45	6.33	8.29	FM(μ =8.97)
CsMn3As5	1000300005	34	5.19	8.91	FM(μ =5.82)
CsMn3Bi5	1000300007	47	5.68	9.89	FM(μ =8.34)
CsMn3Sn5	1000300010	21	5.34	9.88	FM(μ =5.28)
CsMn3S5	1000300012	23	5.74	7.34	FM(μ =10.15)
CsMn3Se5	1000300013	23	5.97	7.62	FM(μ =10.31)
CsFe3Sb5	1000300017	23	5.42	9.59	FM(μ =6.73)
CsCo3Ge5	1000300031	34	4.94	9.23	
CsCo3Sn5	1000300032	21	5.27	9.92	
CsNi3Pb5	1000300044	42	5.45	10.15	
CsNb3Sb5	1000300061	30	5.82	9.63	
CsBi5Rh3	1000300106	21	5.82	9.99	
CsTa3Bi5	1000300139	37	5.91	9.85	
CsPt3Pb5	1000300198	30	5.79	9.73	